

## 基于琥珀酸配体的锌/镉配合物的合成、结构及性质

吕莹<sup>\*1</sup> 李秀梅<sup>1</sup> 黄艳菊<sup>1</sup> 刘博<sup>\*2</sup> 周实<sup>2</sup>

(<sup>1</sup>通化师范学院化学学院, 通化 134002)

(<sup>2</sup>吉林师范大学环境友好材料制备与应用省部共建教育部重点实验室, 四平 136000)

**摘要:** 在水热条件下获得了2个过渡金属配合物 $[\text{Zn}(\text{suc})(\text{HL})]_n$  (**1**)和 $[\text{Cd}(\text{suc})_{0.5}(\text{L})]_n$  (**2**) ( $\text{H}_2\text{suc}$ =琥珀酸,  $\text{HL}$ =3-(2-吡啶基)吡唑), 并通过元素分析、IR光谱、单晶X射线衍射、热重分析、荧光光谱和粉末X射线衍射对结构进行了表征。在配合物**1**中, 羧基配体 $\text{suc}^{2-}$ 通过双齿和单齿模式桥联金属中心形成了二维网络结构。在**2**中,  $\text{suc}^{2-}$ 和L<sup>-</sup>配体连接Cd(II)离子也形成了二维框架。此外, 通过基于Gaussian16程序的PBE0/LANL2DZ方法, 对从**1**和**2**的晶体结构中选出的“分子碎片”进行了量子化学计算。计算结果表明, 配位原子与Zn(II)离子、Cd(II)离子之间存在着明显的共价相互作用。

**关键词:** 锌(II)配合物; 镉(II)配合物; 琥珀酸; 3-(2-吡啶基)吡唑; 晶体结构

中图分类号: O614.24<sup>1</sup>; O614.24<sup>2</sup> 文献标识码: A 文章编号: 1001-4861(2022)12-2511-10

DOI: 10.11862/CJIC.2022.246

## Synthesis, Structure, and Properties of Zinc/Cadmium Complexes Based on Succinic Acid Ligand

LÜ Ying<sup>\*1</sup> LI Xiu-Mei<sup>1</sup> HUANG Yan-Ju<sup>1</sup> LIU Bo<sup>\*2</sup> ZHOU Shi<sup>2</sup>

(<sup>1</sup>Faculty of Chemistry, Tonghua Normal University, Tonghua, Jilin 134002, China)

(<sup>2</sup>Key Laboratory of Preparation and Applications of Environmental Friendly Materials  
(Jilin Normal University), Ministry of Education, Siping, Jilin 136000, China)

**Abstract:** Two transition-metal complexes,  $[\text{Zn}(\text{suc})(\text{HL})]_n$  (**1**) and  $[\text{Cd}(\text{suc})_{0.5}(\text{L})]_n$  (**2**) ( $\text{H}_2\text{suc}$ =succinic acid,  $\text{HL}$ =3-(2-pyridyl)pyrazole), have been achieved under hydrothermal conditions and structurally characterized by elemental analysis, IR spectrum, single-crystal X-ray diffraction, thermogravimetric analysis, fluorescent spectroscopy, and powder X-ray diffraction. In complex **1**, the carboxyl ligand  $\text{suc}^{2-}$  bridges the metal centers via bidentate and monodentate modes. The metal centers are coordinated by  $\text{suc}^{2-}$  to form a 2D network structure. In **2**,  $\text{suc}^{2-}$  and L<sup>-</sup> ligands linked the Cd(II) ions to form a 2D framework too. Besides, the quantum-chemical calculations were finished on ‘molecular fragments’ selected from the crystal structure of **1** and **2** by the PBE0/LANL2DZ method in the Gaussian16 program. The calculation results indicate the distinct covalent interaction between the coordinated atoms and Zn(II) ion/Cd(II) ion. CCDC: 2107594, **1**; 2162815, **2**.

**Keywords:** Zn(II) complex; Cd(II) complex; succinic acid; 3-(2-pyridyl)pyrazole; crystal structure

收稿日期: 2022-06-08。收修改稿日期: 2022-10-15。

吉林省科技发展计划(No.JJKH20210541KJ)资助。

\*通信联系人。E-mail: lvying719@126.com, 112363305@qq.com

## 0 Introduction

Recently, a growing number of interests have been focused on the design strategies and construction of architecture with diverse topologies in supramolecular chemistry and crystal engineering<sup>[1-6]</sup>. As we know, properties are derived from the natural structure, and also can be subtly moderated by slight structure changes<sup>[7]</sup>. It is well known that product topology can often be controlled and modulated. Admirable synthetic strategies have been developed for these new types of entanglement in recent years. It is well known that the resulting structures are determined by several factors, including the coordination geometry of the central metal ions, ligand structure, solvents, metal-ligand ratio, pH value, counterions, and so on<sup>[8-10]</sup>. With this understanding, one crucial aim of this work is to explore the essential factors of positional isomeric ligands for regulating the structural assembly, which may provide further insight into designing new hybrid crystalline materials<sup>[11-15]</sup>. Among these factors, the counterion and solvent effects on the self-assembly process are particularly of interest to give rise to a variety of self-assembled products. Meanwhile, solvents often affect the coordination behavior of the metal ions, which may determine the connectivity and dimensionality of the overall network. Guest solvent molecules can also affect the thermal stabilities via intermolecular interactions with the parent frameworks. Therefore, systematic investigation of an assembling system with fixed metal centers and coordinated organic molecules is crucial for gaining the expected target product<sup>[16-17]</sup>. Hydrogen bonds remain the most reliable and widely used means of enforcing molecular recognition. Besides these conventional strong hydrogen bonds, varieties of unconventional intermolecular contacts (carbonyl $\cdots\pi$ ,  $\pi\cdots\pi$ , and anion $\cdots\pi$ ) have also been found to be instrumental in determining the supramolecular structure of solids<sup>[18-20]</sup>. Meanwhile, pyridyl-pyrazole ligands as neutral pyridine derivatives are deemed excellent organic building blocks. Among various pyridyl-pyrazole ligands, the 3-(2-pyridyl)pyrazole (HL) ligand displays attractive merits<sup>[21-22]</sup>. First, they exhibit good coordination ability

during assembly with metal ions. In the next place, due to a semi-rigid organic skeleton, they have different conformations and good supporting power. As is well known, the coordination polymers (CPs) containing Zn(II)/Cd(II) often exhibit fluorescent, appealing applications in luminescence<sup>[14-15,18,23]</sup>. Therefore, it is of important significance to investigate the effect of carboxylate and pyridine-pyrazole ligands in adjusting the structures of Zn(II) and Cd(II) CPs.

Based on the above-mentioned considerations, semi-rigid HL and flexible succinic acid (H<sub>2</sub>suc) were selected to react with Zn(II) and Cd(II) cations in hydrothermal conditions. As a result, two new 2D complexes of [Zn(suc)(HL)]<sub>n</sub> (**1**) and [Cd(suc)<sub>0.5</sub>(L)]<sub>n</sub> (**2**) were obtained and structurally characterized by elemental analysis techniques, IR, powder X-ray diffraction (PXRD), thermogravimetric analysis (TGA), single-crystal X-ray diffraction, fluorescence spectrum, and quantum-chemical calculations.

## 1 Experimental

### 1.1 Material and methods

All reagents and solvents were used as received from commercial sources and no further purification was made. Elemental analyses (C, H, and N) were carried out using a Vario EL cube elemental analyzer. PXRD data were measured on a D/teX Ultra diffractometer (radiation source: Cu K $\alpha$ ,  $\lambda$ =0.154 184 nm, voltage: 40 kV, current: 40 mA, scan range: 5°-90°). IR absorption spectra (KBr pellet) were recorded on a Varian 640 FTIR spectrometer within the scope of 400-4 000 cm<sup>-1</sup>. Fluorescence spectra were obtained on a Hitachi F-7000 fluorescence spectrometer at 296 K.

### 1.2 Synthesis of the complex

A solution of Zn(NO<sub>3</sub>)<sub>2</sub>·6H<sub>2</sub>O (0.059 5 g, 0.2 mmol), HL (0.029 0 g, 0.2 mmol) and H<sub>2</sub>suc (0.023 6 g, 0.20 mmol) in 6 mL water and 4 mL 0.1 mol·L<sup>-1</sup> NaOH was transferred into a 25 mL Teflon-lined autoclave and kept at 150 °C for 168 h. After slowly cooling to room temperature for one day, yellow block crystals of complex **1** were gained. Yield: 23% based on HL. Anal. Calcd. for C<sub>12</sub>H<sub>11</sub>N<sub>3</sub>O<sub>4</sub>Zn(%): C, 44.12; H, 3.39; N, 12.86. Found(%): C, 43.98; H, 3.07; N, 12.49. IR

(KBr pellet,  $\text{cm}^{-1}$ ): 3 423m, 3 113w, 2 958w, 2 928w, 1 599s, 1 477m, 1 452m, 1 426s, 1 364m, 1 336w, 1 277w, 1 216w, 1 145s, 1 128s, 1 090w, 1 072m, 1 033w, 1 048w, 1 033w, 1 002w, 984w, 972w, 954w, 792w, 757s, 711m, 698w, 683w, 668w, 650w, 627w, 501w, 470m, 442w.

A solution of  $\text{Cd}(\text{OAc})_2 \cdot 2\text{H}_2\text{O}$  (0.053 0 g, 0.2 mmol), HL (0.029 0 g, 0.2 mmol) and  $\text{H}_2\text{suc}$  (0.023 6 g, 0.20 mmol) in 6 mL water and 4.5 mL  $0.1 \text{ mol} \cdot \text{L}^{-1}$  NaOH was transferred into a 25 mL Teflon-lined autoclave and kept at  $150 \text{ }^\circ\text{C}$  for 168 h. After slowly cooling to room temperature for one day, yellow block crystals of complex **2** were gained. Yield: 27% based on HL. Anal. Calcd. for  $\text{C}_{10}\text{H}_8\text{CdN}_3\text{O}_2$ (%): C, 38.18; H, 2.56; N, 13.36. Found(%): C, 37.82; H, 2.12; N, 12.98. IR (KBr pellet,  $\text{cm}^{-1}$ ): 3 429w, 3 105w, 2 931w, 1 601s, 1 553m, 1 468w, 1 451m, 1 429m, 1 380m, 1 351w, 1 279w, 1 216w, 1 151w, 1 165m, 1 115m, 1 092w, 1 066w, 1 050w, 1 012w, 973w, 990w, 880w, 779w, 746s,

710m, 695w, 683w, 662w, 637w, 511w.

### 1.3 Single-crystal data collection and structure determination

Two single crystals with dimensions of  $0.15 \text{ mm} \times 0.12 \text{ mm} \times 0.10 \text{ mm}$  (**1**) and  $0.21 \text{ mm} \times 0.15 \text{ mm} \times 0.10 \text{ mm}$  (**2**) were collected at 293(2) K on an Oxford Diffraction Gemini R Ultra diffractometer with  $\text{Mo } K\alpha$  ( $\lambda = 0.071 073 \text{ nm}$ ). The structures were solved by direct methods using the SHELXS-97 program of the SHELXL - 97 crystallographic software package and refined on  $F^2$  by full-matrix least-squares methods. All non-hydrogen atoms were refined anisotropically. All the hydrogen atoms were positioned geometrically and refined using a riding model. A summary of the crystallography data and structure refinements for **1** and **2** is given in Table 1. The selected bond lengths and angles for complexes **1** and **2** are listed in Table 2. The hydrogen bond parameters of complex **1** are given in Table 3.

CCDC: 2107594, **1**; 2162815, **2**.

Table 1 Crystal data for complexes **1** and **2**

Parameter	<b>1</b>	<b>2</b>
Empirical formula	$\text{C}_{12}\text{H}_{11}\text{N}_3\text{O}_4\text{Zn}$	$\text{C}_{10}\text{H}_8\text{CdN}_3\text{O}_2$
Formula weight	326.61	314.59
Crystal system	Monoclinic	Monoclinic
Space group	$P2_1/c$	$C2/c$
$a / \text{nm}$	0.794 00(5)	2.399 33(15)
$b / \text{nm}$	1.964 77(12)	0.677 85(4)
$c / \text{nm}$	0.780 43(5)	1.344 90(8)
$\beta / (^\circ)$	96.088 0(10)	114.364(2)
Volume / $\text{nm}^3$	1.210 63(13)	1.992 5(2)
$Z$	4	8
$F(000)$	664	1 224
$D_c / (\text{g} \cdot \text{cm}^{-3})$	1.792	2.097
GOF	0.948	1.055
Reflection collected, unique	8 059, 2 230	7 864, 2 418
$R_{\text{int}}$	0.049 6	0.020 8
$R_1 [I > 2\sigma(I)]$	0.027 9	0.018 3
$wR_2$	0.069 1	0.042 7

Table 2 Selected bond distances (nm) and angles ( $^\circ$ ) for complexes **1** and **2**

<b>1</b>					
Zn1—O1	0.198 27(15)	Zn1—O3a	0.215 18(16)	Zn1—O4b	0.199 92(16)
Zn1—N1	0.213 69(19)	Zn1—N2	0.214 32(19)		
O3—Zn1—O4b	117.59(7)	O1—Zn1—N1	132.95(7)	O4b—Zn1—N1	109.46(7)

Continued Table 2

O1—Zn1—N2	96.36(7)	O4b—Zn1—N2	97.36(7)	N1—Zn1—N2	76.53(7)
O1—Zn1—O3a	86.75(6)	O4b—Zn1—O3a	89.25(7)	N1—Zn1—O3a	94.62(7)
N2—Zn1—O3a	170.31(7)				
<b>2</b>					
Cd1—O1	0.229 69(13)	Cd1—O1a	0.243 85(15)	Cd1—O2b	0.242 78(15)
Cd1—N1a	0.222 40(16)	Cd1—N2	0.235 19(16)	Cd1—N3	0.234 96(17)
N1a—Cd1—O1	103.93(6)	N1a—Cd1—N3	167.96(6)	O1—Cd1—N3	87.95(6)
N1—Cd1—N2	97.36(6)	O1—Cd1—N2	157.28(5)	N3—Cd1—N2	71.17(6)
O1—Cd1—O2b	98.10(5)	N3—Cd1—O2b	78.85(5)	N2—Cd1—O2b	86.82(5)
O1—Cd1—O1a	70.63(5)	N3—Cd1—O1a	89.21(5)	N2—Cd1—O1a	99.44(5)

Symmetry codes: a:  $x-1, y, z$ ; b:  $x-1, -y+1/2, z-1/2$  for **1**; a:  $x+1, -y, z-1/2$ ; b:  $x+1, 1-y, z-1/2$  for **2**.

Table 3 Selected hydrogen bond parameters for complex **1**

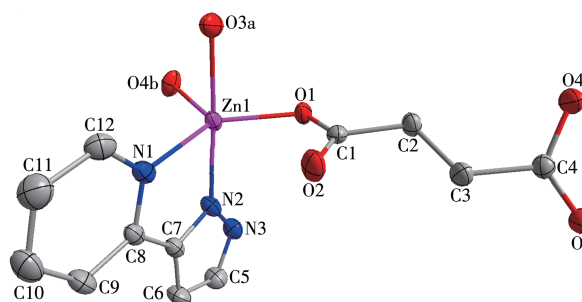
D—H $\cdots$ A	$d(\text{D—H}) / \text{nm}$	$d(\text{H}\cdots\text{A}) / \text{nm}$	$d(\text{D}\cdots\text{A}) / \text{nm}$	$\angle\text{DHA} / (^\circ)$	Symmetry code
N3—H3A $\cdots$ O1	0.086	0.187	0.272 7(3)	176	$x, 1/2-y, -1/2+z$
C5—H5A $\cdots$ O2	0.093	0.243	0.330 0(3)	155	$x, y, -1+z$
C6—H6A $\cdots$ O2	0.093	0.239	0.326 8(3)	157	$-x, -y, -z$
C9—H9A $\cdots$ O2	0.093	0.268	0.347 6(3)	161	$-x, -y, -z$

## 2 Results and discussion

### 2.1 Structural description

The single-crystal X-ray study reveals that complex **1** is a 3D supramolecular structure based on a 2D network complex. There are one crystallographically independent Zn(II) cation, one HL molecule, and one  $\text{suc}^{2-}$  anion, as displayed in Fig.1. The central Zn1 cation is five-coordinated by two nitrogen atoms from one HL molecule and three carboxylic oxygen atoms of three  $\text{suc}^{2-}$  anions. The Zn—N bond distances are in a range of 0.213 69(19)-0.214 32(19) nm, and the Zn—O bond lengths lie in the 0.198 27(15)-0.215 18(16) nm range. The bond angles around Zn(II) cations vary from  $76.53(7)^\circ$  to  $170.31(7)^\circ$ , indicating that the trigonal bipyramid is slightly distorted. In complex **1**, HL shows a bidentate coordination mode, which is different from the reported complex<sup>[21]</sup>. In the  $\text{suc}^{2-}$  anion, one carboxylic group coordinates with one Zn(II) ion in a monodentate coordination mode, and other coordinates with two Zn(II) ions in a bidentate coordination mode to form a 2D network structure with an 18-membered ring (Fig.2). Finally, the 2D network is extended into a 3D supramolecular architecture by hydrogen bonds between the N atoms, C atoms of HL and carboxylic oxygen atoms of

$\text{suc}^{2-}$ . The corresponding hydrogen-bonding parameters of complex **1** are given in Table 3. It is worth mentioning that there are  $\pi \cdots \pi$  interactions in complex **1** between the pyrazole and pyridine rings, pyridine rings of HL molecules (Fig.3). The centroid-to-centroid distances between adjacent rings are 0.382 85(15) nm for N2N3C5C6C7 pyrazole ring and N1C8C9C10C11 pyridine ring (Symmetry code:  $2-x, -y, -z$ ) and 0.366 32(15) nm for N1C8C9C10C11 and N1aC8aC9a C10aC11a pyridine rings (Symmetry code:  $1-x, -y, -z$ ). The dihedral angles are  $2.66(14)^\circ$  and  $0.00(12)^\circ$ , respectively. Generally speaking, organic dicarboxylate and pyridyl-pyrazole are two kinds of well-bridged



Symmetry codes: a:  $x-1, y, z$ ; b:  $x-1, -y+1/2, z-1/2$

Fig.1 View of coordination environment (at 50% probability level) of Zn(II) ion of complex **1**

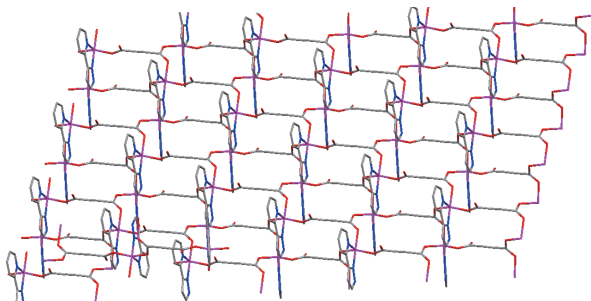
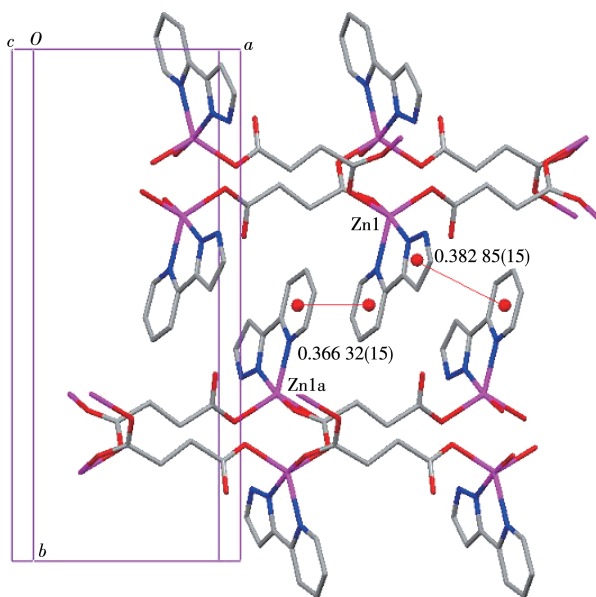


Fig.2 View of the 2D network structure of complex 1

Symmetry code:  $a: x-1, y, z$ Fig.3  $\pi \cdots \pi$  interactions of complex 1

ligands and are usually used to construct 1D, 2D, and 3D coordination polymers. In **1**, HL acts as a terminal-type ligand to form a discrete complex, which is unusual.

Complex **2** crystallizes in the monoclinic  $C2/c$  space group, with one Cd(II) ion, half a  $\text{suc}^{2-}$  anion, and an  $\text{L}^-$  anion in its asymmetric unit (Fig. 4). The six-coordinated Cd(II) center is surrounded by three oxygen atoms (O1, O1a, O2b) from three different  $\text{suc}^{2-}$  anions, three nitrogen atoms (N1a, N2, N3) from two different  $\text{L}^-$  anions, adopting a distorted octahedral  $\{\text{CdO}_3\text{N}_3\}$  geometry with Cd—O bond lengths are 0.229 69(13), 0.242 78(15), 0.243 85(15) nm and Cd—N bond distances are 0.222 40(16), 0.234 96(17), and 0.235 19(16) nm, respectively. The O(N)—Cd—N(O) bond angles are in a range of  $70.63(5)^\circ$ – $164.02(5)^\circ$ , all of which are within the reasonable range of those reported for other six-coordinated Cd(II) complexes<sup>[15,22]</sup>. In the polymeric

structure of complex **2** (Fig. 5), the  $\text{suc}^{2-}$  anion adopts the bridging- $\mu_6$  mode to connect six cadmium ions, whereas the  $\text{L}^-$  anion adopts a bridging- $\mu_3$  mode to connect two metal ions. In this manner, an ideal 2D coordination polymer with two-nuclear structure along the  $a$ -axis has been built.

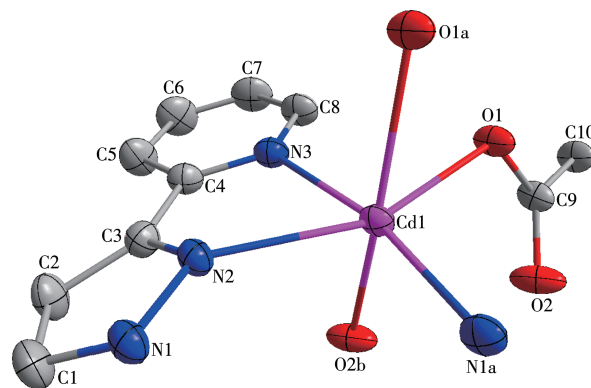
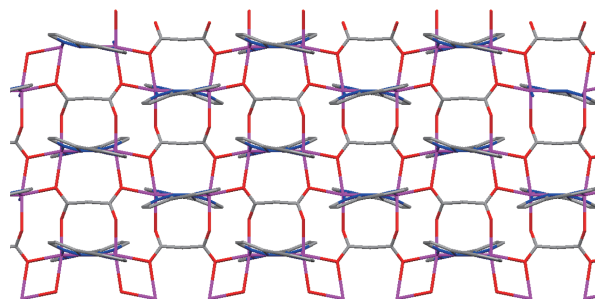
Symmetry codes:  $a: x+1, -y, z-1/2$ ;  $b: x+1, 1-y, z-1/2$ 

Fig.4 View of coordination environment (at 50% probability level) of Cd(II) ion of complex 2

Fig.5 View of the 2D network structure of complex 2 along the  $a$ -axis

It should be noted that all the nitrogen atoms of  $\text{L}^-$  in complex **2** have been involved in the coordination. As a result, it serves to balance the charge. However, only two nitrogen atoms of HL in complex **1** are involved in the coordination and there is no need to balance the charge.

## 2.2 IR spectrum analysis

IR spectrum of **1** is exhibited in the wavenumber range of 4 000 to 400  $\text{cm}^{-1}$  (Fig.S1, Supporting information). The strong band at about 1 599  $\text{cm}^{-1}$  is attributed to the  $\nu_{\text{C=O}}$  vibration of the groups of  $\text{suc}^{2-}$ <sup>[24]</sup>. The peak located at 1 452  $\text{cm}^{-1}$  is identified as the stretching vibration of carboxylic groups<sup>[25]</sup>. The strong bands in the region of 668–757  $\text{cm}^{-1}$  can be vested in the  $\nu_{\text{C-N}}$

vibration of the N-heterocyclic rings of HL<sup>[26]</sup>.

IR spectrum of **2** is exhibited in the wavenumber range of 4 000 to 400 cm<sup>-1</sup> (Fig.S2). The strong band at about 1 601 cm<sup>-1</sup> is attributed to the  $\nu_{C=O}$  vibration of suc<sup>2-</sup><sup>[24]</sup>. The peak located at 1 451 cm<sup>-1</sup> is identified as the stretching vibration of carboxylic groups<sup>[25]</sup>. The strong bands in the region of 662 - 746 cm<sup>-1</sup> can be vested in the  $\nu_{C-N}$  vibration of the N-heterocyclic rings of L<sup>-</sup><sup>[26]</sup>.

### 2.3 PXRD and thermal stability analyses

To substantiate the phase purity of complexes **1** and **2**, their PXRD was performed before their photoluminescent properties were measured. The experimental PXRD patterns were in good agreement with the corresponding simulated ones (Fig.6) except for the relative intensity variation because of the preferred orientations

of the crystals.

Complexes **1** and **2** are stable under environmental conditions, and the thermal stability was explored by TGA. For **1**, there were two separate weight loss steps. The first weight loss of 41.8% occurred at 215-268 °C, which is due to the departure of coordinated HL ligand (Calcd. 44.4%). The second weight loss of 33.8% from 390 to 600 °C corresponds to the loss of all the remaining suc<sup>2-</sup> anions (Calcd. 35.5%), as shown in Fig. S3. For **2**, the first weight loss of 46.2% occurred at 100-175 °C, which is due to the removal of coordinated L<sup>-</sup> ligand (Calcd. 45.8%). The second weight loss of 34.8% from 175 to 600 °C corresponds to the loss of all the remaining suc<sup>2-</sup> anions (Calcd. 36.9%), as shown in Fig.S4.

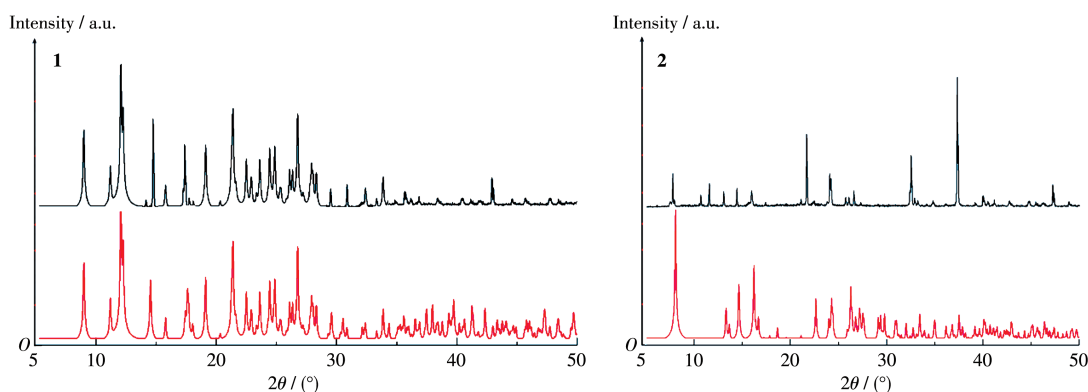


Fig.6 Simulated (bottom) and experimental (top) PXRD patterns of complexes **1** and **2**

### 2.4 Photoluminescent properties

CPs with  $d^{10}$  metal centers have many potential applications such as in chemical sensors, photochemistry, and electroluminescent display<sup>[27]</sup>. Therefore, in the

present work, the photoluminescent properties of HL and complexes **1** and **2** have been investigated in the solid state at room temperature. The emission peaks are shown in Fig. 7, and the solid-state fluorescence

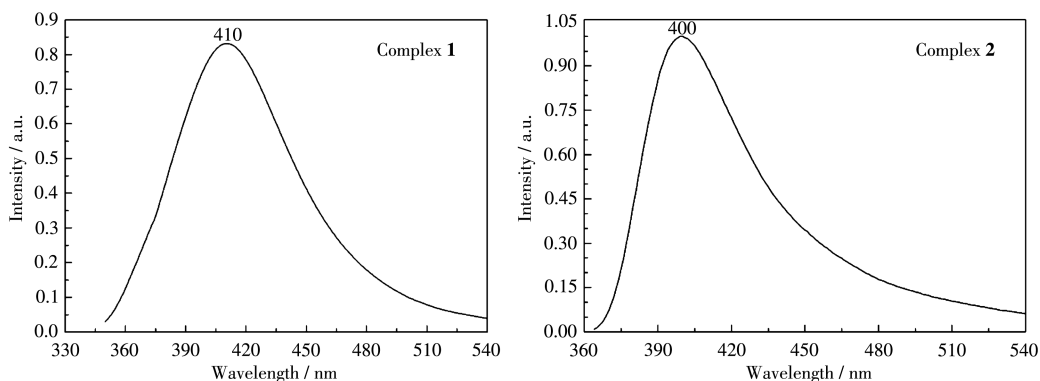


Fig.7 Solid-state luminescence emission spectra of complexes **1** and **2** at room temperature

quantum yield of complex **1** was 20%, while that of complex **2** was 24%.

The main emission peak of H<sub>2</sub>suc is at 258 nm<sup>[28]</sup>. HL show emission peak at 443 nm ( $\lambda_{\text{ex}}=350$  nm). The emission bands of these free ligands are probably caused by the  $\pi^* \rightarrow n$  or  $\pi^* \rightarrow \pi$  transition<sup>[29]</sup>. Upon complexation of these ligands with Zn(II)/Cd(II) ions, the emission peaks occurred at 410 nm ( $\lambda_{\text{ex}}=294$  nm) for **1** and 400 nm ( $\lambda_{\text{ex}}=335$  nm) for **2**. For complexes **1** and **2**, the main emission peaks were highly blue-shifted by 33 and 43 nm with respect to the free HL, respectively. Because the Zn(II) and Cd(II) ions are difficult to oxidize or reduce due to the  $d^{10}$  configuration, the emissions of the complexes are neither MLCT nor LMCT in nature<sup>[30]</sup>. As a result, the emission can be assigned to intraligand transitions<sup>[31]</sup>.

## 2.5 Theoretical calculations

All calculations were accomplished by the Gaussian16 program. The parameters of the molecular fragments used for calculations were extracted from the crystal structure of complexes **1** and **2**, respectively. Furthermore, we explained natural bond orbital (NBO) by density functional theory (DFT)<sup>[32]</sup> using the PBE0<sup>[33]</sup> hybrid functional and the LANL2DZ basis set<sup>[34]</sup>.

In Table 4, we summarize the selected net

charges, natural electron configurations, Wiberg bond indexes, and NBO bond orders for **1**. Clearly, the electronic configurations of Zn1, N and O atoms are  $4s^{0.31}3d^{9.98}4p^{0.40}$ ,  $2s^{1.33-1.37}2p^{3.65-4.19}$ , and  $2s^{1.68}2p^{4.99-5.14}$ , respectively. Based on the above understanding, the Zn1 atom coordination with N and O atoms is mainly on  $3d$ ,  $4s$  and  $4p$  orbitals. The N atoms use  $2s$  and  $2p$  orbitals to form coordination bonds with the Zn1 atom. All O atoms provide  $2s$  and  $2p$  electrons to the Zn1 atom and form coordination bonds. Consequently, the Zn1 atom obtains some electrons from two nitrogen atoms of HL and three oxygen atoms of  $\text{suc}^{2-}$ <sup>[35-36]</sup>. Accordingly, in light of valence-bond theory, the atomic net charge distribution and NBO bond orders of **1** (Table 4) show obvious covalent interaction between the coordinated atoms and Zn(II) ion. The differences in the NBO bond orders for Zn—O and Zn—N make their bond lengths different, which is in good agreement with the X-ray crystal structure data of **1**.

As can be seen in Fig.8, the HOMO of **1** is mainly composed of  $\text{suc}^{2-}$ . Nevertheless, the LUMO mainly consists of HL. Therefore, the ligand-to-ligand charge transfer (LLCT) may be concluded from some contours of molecular orbitals of **1**.

Similar parameters of **2** are also listed in Table 4.

**Table 4** Natural atomic charges, natural valence electron configurations, Wiberg bond indexes, and NBO bond orders for complexes **1** and **2**

Atom	Net charge	Electron configuration	Bond	Wiberg bond index	NBO bond order / a.u.
<b>1</b>					
Zn1	1.307 68	[core]4s <sup>0.31</sup> 3d <sup>9.98</sup> 4p <sup>0.40</sup>			
O1	-0.788 84	[core]2s <sup>1.68</sup> 2p <sup>5.05</sup>	Zn1—O1	0.259 8	0.308 8
O3a	-0.684 19	[core]2s <sup>1.68</sup> 2p <sup>4.99</sup>	Zn1—O3a	0.179 8	0.239 2
O4b	-0.830 31	[core]2s <sup>1.68</sup> 2p <sup>5.14</sup>	Zn1—O4b	0.249 6	0.300 9
N1	-0.537 74	[core]2s <sup>1.33</sup> 2p <sup>4.19</sup>	Zn1—N1	0.182 6	0.279 8
N2	-0.345 84	[core]2s <sup>1.37</sup> 2p <sup>3.95</sup>	Zn1—N2	0.169 6	0.271 0
<b>2</b>					
Cd1	1.414 83	[core]5s <sup>0.30</sup> 4d <sup>9.98</sup> 5p <sup>0.29</sup>			
N1a	-0.437 19	[core]2s <sup>1.41</sup> 2p <sup>4.00</sup>	Cd1—N1a	0.151 6	0.217 0
N2	-0.468 08	[core]2s <sup>1.38</sup> 2p <sup>4.06</sup>	Cd1—N2	0.155 7	0.216 9
N3	-0.545 84	[core]2s <sup>1.33</sup> 2p <sup>4.19</sup>	Cd1—N3	0.117 4	0.182 2
O1	-0.766 27	[core]2s <sup>1.71</sup> 2p <sup>5.05</sup>	Cd1—O1	0.172 0	0.197 7
O1a	-0.658 52	[core]2s <sup>1.71</sup> 2p <sup>4.94</sup>	Cd1—O1a	0.127 9	0.167 1
O2b	-0.628 87	[core]2s <sup>1.69</sup> 2p <sup>4.92</sup>	Cd1—O2b	0.121 5	0.161 4

Symmetry codes: a: x-1, y, z; b: x-1, -y+1/2, z-1/2 for **1**; a: x+1, -y, z-1/2; b: x+1, 1-y, z-1/2 for **2**.

We can see that the electronic configurations of Cd1, N, and O atoms are  $5s^{0.30}4d^{9.98}5p^{0.29}$ ,  $2s^{1.33-1.41}2p^{4.00-4.19}$ , and  $2s^{1.69-1.71}2p^{4.92-5.05}$ , respectively. From this, we can conclude that the Cd1 atom coordination with N and O atoms is mainly on  $4d$ ,  $5s$ , and  $5p$  orbitals. All N atoms and O atoms form coordination bonds with Cd(II) ion using  $2s$  and  $2p$  orbitals. Consequently, the Cd1 atom obtains some electrons from the N atoms of  $L^-$  and O

atoms of  $suc^{2-}$ [35-36]. Thus, according to valence-bond theory, the atomic net charge distribution in **2** shows the obvious covalent interaction between the coordinated atoms and the Cd1 atom. As can be seen from Fig.9, the HOMO mainly consists of  $suc^{2-}$ , while the LUMO is mainly composed of  $suc^{2-}$  and HL. So, the LLCT and intramolecular charge transfer (ILCT) may be inferred from some contours of molecular orbitals of **2**.

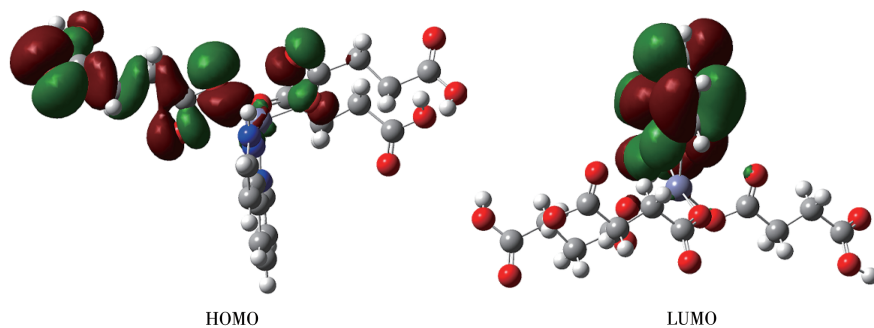


Fig.8 Frontier molecular orbitals of complex **1**

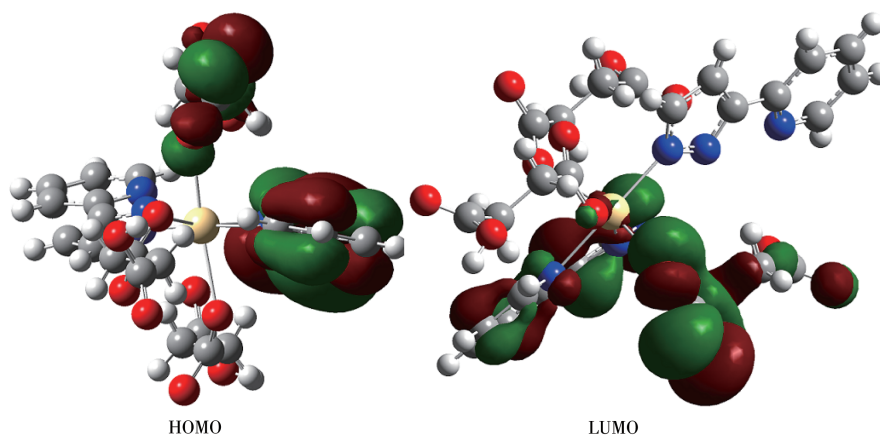


Fig.9 Frontier molecular orbitals of complex **2**

### 3 Conclusions

Two new complexes based on succinic acid were successfully synthesized by the hydrothermal method. They are also structurally characterized by elemental analysis techniques, IR, PXRD, TGA, single-crystal X-ray diffraction, fluorescence spectrum, and quantum-chemical calculations. The complexes have the 2D network structure formed by metal ions and the ligands connecting infinitely in a carboxyl bridging manner.

Supporting information is available at <http://www.wjhxzb.cn>

### References:

- [1] Li H L, Eddaoudi M, O'Keeffe M, Yaghi O M. Design and Synthesis of an Exceptionally Stable and Highly Porous Metal-Organic Framework. *Nature*, **1999**,**402**:276-279
- [2] Ge J Y, Chen Z Y, Zhang L, Liang X, Xu J, Kurmoo M, Zuo J L. A Two-Dimensional Iron(II) Coordination Polymer with Synergetic Spin-Crossover and Luminescent Properties. *Angew. Chem. Int. Ed.*, **2019**, **58**(26):8789-8793
- [3] Shi C, Zhang M, Hang X X, Bi Y F, Huang L L, Zhou K, Xu Z H, Zheng Z P. Assembly of Thiacalix[4]Arene-Supported High-Nuclearity  $Cd_{24}$  Cluster with Enhanced Photocatalytic Activity. *Nanoscale*, **2018**, **10**(30):14448-14454
- [4] Zhang M, Chen M W, Bi Y F, Huang L L, Zhou K, Zheng Z P. A

- Bimetallic Co<sub>4</sub>Mo<sub>8</sub> Cluster Built from Mo<sub>8</sub> Oxothiomolybdate Capped by a Co<sub>4</sub>-Thiacalix[4]arene Unit: The Observation of the Co-Mo Synergistic Effect for Binder-Free Electrocatalysts. *J. Mater. Chem. A*, **2019**, *7*(20):12893-12899
- [5] Liu C, Jiang W, Hu F, Wu X, Xue D F. Mesoporous NiCo<sub>2</sub>O<sub>4</sub> Nanoneedle Arrays as Supercapacitor Electrode Materials with Excellent Cycling Stabilities. *Inorg. Chem. Front.*, **2018**, *5*(4):835-843
- [6] Cui J W, Hou S X, Li Y H, Cui G H. A Multifunctional Ni(II) Coordination Polymer: Synthesis, Crystal Structure and Applications as a Luminescent Sensor, Electrochemical Probe, and Photocatalyst. *Dalton Trans.*, **2017**, *46*(48):16911-16924
- [7] Meng F Y, Zhou Y L, Zou H H, Zeng M H, Liang H. Solution and Solid-State Photoluminescence of Bis[succinatobis[2,6-bis(2-benzimidazolyl)]Lead(II)]: A Comment on the Lone-pair Stereochemistry and Its Effect on Supramolecular Interaction. *J. Mol. Struct.*, **2009**, *920*(1/2/3):238-241
- [8] Cui L S, Meng X M, Li Y G, Huang K R, Li Y C, Long J Q, Yao P F. Syntheses, Structural Diversity, and Photocatalytic-Degradation Properties for Methylene Blue of Co(II) and Ni(II) MOFs Based on Terephthalic Acid and Different Imidazole Bridging Ligands. *CrystEngComm*, **2019**, *21*(25):3798-3809
- [9] Gao Q, Xu J, Bu X H. Recent Advances about Metal-Organic Frameworks in the Removal of Pollutants from Wastewater. *Coord. Chem. Rev.*, **2019**, *378*:17-31
- [10] Li C, Deng Z P, Huo L H, Gao S. Cooperative Effects of Metal Cations and Coordination Modes on Luminescent s-Block Metal-Organic Complexes Constructed from V-Shaped 4,4'-Sulfonyldiphenol. *CrystEngComm*, **2018**, *20*(46):7513-7525
- [11] Zhang H, Ji L Q, Song Y Z, Kong Z G, Li C, Wang X Y. Syntheses, Crystal Structures and Properties of Mn(II) and Co(II) Coordination Complexes Based on 1,10-Phenanthroline Derivative. *Chin. J. Struct. Chem.*, **2021**, *40*(3):336-342
- [12] Vizuet J P, Howlett T S, Lewis A L, Chroust Z D, McCandless G T, Balkus K J. Transition from a 1D Coordination Polymer to a Mixed-Linker Layered MOF. *Inorg. Chem.*, **2019**, *58*(8):5031-5041
- [13] Liu G C, Li Y, Chi J, Xu N, Wang X L, Lin H Y, Chen Y Q. Multifunctional Fluorescent Responses of Cobalt Complexes Derived from Functionalized Amide-Bridged Ligand. *Dyes Pigment.*, **2020**, *174*:108064
- [14] Pan Y R, Li X M, Liu B, Zhou S, Chang Y F. Two New Zn(II) and Co(II) Coordination Polymers Constructed by 4-Bromobenzoic Acid and 1,4-Bis(imidazol-1-yl)-butane: Synthesis, Crystal Structure and Theoretical Calculations. *Chin. J. Struct. Chem.*, **2019**, *38*(4):635-643
- [15] 李秀梅, 潘亚茹, 刘博, 周实. 两个由双咪唑基配体构筑的镉配合物的合成、晶体结构及理论计算. *无机化学学报*, **2019**, *35*(7):1275-1282  
LI X M, PAN Y R, LIU B, ZHOU S. Syntheses, Crystal Structures and Theoretical Calculations of Two Cadmium(II) Complexes Assembled by Bis(imidazol) Ligands. *Chinese J. Inorg. Chem.*, **2019**, *35*(7):1275-1282
- [16] Kirchon A, Feng L, Drake H F, Joseph, E A, Zhou H C. From Fundamentals to Applications: A Toolbox for Robust and Multifunctional MOF Materials. *Chem. Soc. Rev.*, **2018**, *47*(23):8611-8638
- [17] Fang W H, Yang G Y. Induced Aggregation and Synergistic Coordination Strategy in Cluster Organic Architectures. *Acc. Chem. Res.*, **2018**, *51*(11):2888-2896
- [18] Huang F P, Zhang Q, Yu Q, Liang H, Yan S P, Liao D Z, Cheng P. Coordination Assemblies of Co<sup>II</sup>/Ni<sup>II</sup>/Zn<sup>II</sup>/Cd<sup>II</sup> with Succinic Acid and Bent Connectors: Structural Diversity and Spin-Canted Antiferromagnetism. *Cryst. Growth Des.*, **2012**, *12*(4):1890-1898
- [19] Gong C H, Guo H Y, Zeng X H, Xu H, Zeng Q D, Zhang J Y, Xie J L. Flexible and Rigid Dicarboxylic Acids Enable the Assembly of Achiral and Chiral 3D Co(II) Metal-Organic Frameworks. *Dalton Trans.*, **2018**, *47*(20):6917-6923
- [20] Wang J, Wei J, Guo F W, Li C Y, Zhu P F, Zhu W H. Homochiral 3D Coordination Polymer with Unprecedented Three-Directional Helical Topology from Achiral Precursor: Synthesis, Crystal Structure, and Luminescence Properties of Uranyl Succinate Metal-Organic Framework. *Dalton Trans.*, **2015**, *44*(31):13809-13813
- [21] Gao Y X, Li X M, Zhou S, Liu B. Synthesis, Structure and Theoretical Calculation of Metal Coordination Polymers with Pyrazine-2,3-dicarboxylic Acid and 3-(2-Pyridyl)pyrazole as Co-ligands. *Chin. J. Struct. Chem.*, **2021**, *40*(6):753-758
- [22] Wang X Y, Li X M, Pan Y R, Liu B, Zhou S. A New Three-dimensional Cd(II) Complex Assembled by 1,3,5-Benzenetricarboxylic Acid and 3-(2-Pyridyl)pyrazole. *Chin. J. Struct. Chem.*, **2019**, *38*(8):1275-1282
- [23] Liu G C, Han S W, Gao Y, Wang X L, Chen B K. Multifunctional Fluorescence Responses of Phenyl-Amide-Bridged d<sup>10</sup> Coordination Polymers Structurally Regulated by Dicarboxylates and Metal Ions. *CrystEngComm*, **2020**, *22*(45):7952-7961
- [24] Yang L, Wang F, Auphedeous D Y, Feng C L. Achiral Isomers Controlled Circularly Polarized Luminescence in Supramolecular Hydrogels. *Nanoscale*, **2019**, *11*:14210-14215
- [25] Wang X L, Mu B, Lin H Y, Liu G C. Three New Two-Dimensional Metal-Organic Coordination Polymers Derived from Bis(pyridinecarboxamide)-1,4-benzene Ligands and 1,3-Benzenedicarboxylate: Syntheses and Electrochemical Property. *J. Organomet. Chem.*, **2011**, *696*(11/12):2313-2321
- [26] Dolensky B, Konvalinka R, Jakubek M, Kral V. Identification of Intramolecular Hydrogen Bonds as the Origin of Malfunctioning of Multitopic Receptors. *J. Mol. Struct.*, **2013**, *1035*:124-128
- [27] McGarrah J E, Kim Y J, Hissler M, Eisenberg R. Toward a Molecular Photochemical Device: A Triad for Photoinduced Charge Separation Based on a Platinum Diimine Bis(acetylide) Chromophore. *Inorg. Chem.*, **2001**, *40*(18):4510-4511
- [28] 谭慧, 王丽影, 周悦, 苟丽宁, 吴盘亮, 郭栋才. 钽-芳香化合物-丁二酸发光配合物的合成及性能. *发光学报*, **2009**, *30*(1):101-107  
TAN H, WANG L Y, ZHOU Y, GOU L N, WU P L, GUO D C. Synthesis and Properties of Terbium-Aromatic Compound-Butyric Acid Luminous Complex. *Chinese Journal of Luminescence*, **2009**, *30*(1):101-107

- [29] Lin J D, Long X F, Lin P, Du S W. A Series of Cation-Templated, Polycarboxylate-Based Cd(II) or Cd(II)/Li(I) Frameworks with Second-Order Nonlinear Optical and Ferroelectric Properties. *Cryst. Growth Des.*, **2010**,**10**(1):146-157
- [30] Lin J G, Zang S Q, Tian Z F, Li Y Z, Xu Y Y, Zhu H Z, Meng Q J. Metal-Organic Frameworks Constructed from Mixed-Ligand 1,2,3,4-Tetra-(4-pyridyl)-butane and Benzene-polycarboxylate Acids: Syntheses, Structures and Physical Properties. *CrystEngComm*, **2007**,**9**(10):915-921
- [31] Liu H Y, Wu H, Ma J F, Liu Y Y, Liu B, Yang J. Syntheses, Structures, and Photoluminescence of Zinc (II) Coordination Polymers Based on Carboxylates and Flexible Bis-[(pyridyl)-benzimidazole] Ligands. *Cryst. Growth Des.*, **2010**,**10**(11):4795-4805
- [32] Parr R G, Yang W. Density Functional Theory of Atoms and Molecules. Oxford: Oxford University Press, **1989**.
- [33] Ernzerhof M, Scuseria G E. Assessment of the Perdew-Burke-Ernzerhof Exchange - Correlation Functional. *J. Chem. Phys.*, **1999**,**110**:5029-5036
- [34] Dunning T H, Hay P J. Gaussian Basis Sets for Molecular Calculations//Schaefer H F. *Methods in Electronic Structure Theory (Modern Theoretical Chemistry)*. New York: Plenum Press, **1977**:1-28
- [35] Wang L, Zhao J, Ni L, Yao J. Synthesis, Structure, Fluorescence Properties, and Natural Bond Orbital (NBO) Analysis of Two Metal [Eu<sup>III</sup>, Co<sup>II</sup>] Coordination Polymers Containing 1,3-Benzenedicarboxylate and 2-(4-Methoxyphenyl)-1*H*-imidazo[4,5-*f*][1,10]phenanthroline Ligands. *Z. Anorg. Allg. Chem.*, **2012**,**638**(1):224-230
- [36] 李章朋, 邢永恒, 张元红, 白凤英, 曾小庆, 葛茂发. 蝎型钒氧苯甲酸配合物的合成、结构及量化计算. *物理化学学报*, **2009**,**25**(4):741-746
- LI Z P, XING Y H, ZHANG Y H, BAI F Y, ZENG X Q, GE M F. Synthesis, Structure and Quantification of Scorpion Vanadium Oxybenzoic Acid Complex. *Acta Phys.-Chim. Sin.*, **2009**,**25**(4):741-746